The response of terrestrial ecosystem carbon cycling under different aerosol-based radiation management geoengineering

Hanna Lee[1], Helene Muri[2], Altug Ekici[1,3,4], Jerry Tjiputra[1], and Jörg Schwinger[1]

[1]NORCE Norwegian Research Institute, Bjerknes Centre for Climate Research, Bergen, Norway
[2]Industrial Ecology Programme, Department of Energy and Process Engineering, Norwegian University of Science and Technology, Trondheim, Norway
[3]Current address: Climate and Environmental Physics, Physics Institute, University of Bern, Bern, Switzerland
[4]Current address: Oeschger Centre for Climate Change Research, University of Bern, Bern, Switzerland

Correspondence: Hanna Lee (hanna.lee@norceresearch.no)

Abstract. Geoengineering has been discussed as a potential option to offset the global impacts of anthropogenic climate change, and at the same time by reaching global temperature targets of the Paris Agreement. Before any implementation of geoengineering, however, the complex natural responses and consequences of such methods should be fully understood to avoid any unexpected and potentially degrading impacts. Here we assess the changes in ecosystem carbon exchange and storage among different terrestrial biomes under three aerosol based radiation management methods with the baseline of RCP8.5 using an Earth System Model (NorESM1-ME). All three methods used in this study (stratospheric aerosol injection, marine sky brightening, cirrus cloud thinning) target the global mean radiation balance at the top of the atmosphere to reach that of the RCP4.5 scenario. The three RM methods investigated in this study show vastly different precipitation patterns especially in the tropical forest biome. Precipitation differences from the three RM methods result large variability in global vegetation carbon uptake and storage. Our findings show that there are unforeseen regional consequences under geoengineering and these consequences should be taken into account in future climate policies as they have substantial impact on terrestrial ecosystems. Although, changes in temperature and precipitation play a large role in vegetation carbon uptake and storage, our results show that CO_2 fertilization also plays a considerable role. We find that the effects of geoengineering on vegetation carbon storage was much smaller than the effects of mitigation under RCP4.5 scenario (e.g. afforestation in the tropics). Our results emphasizes the importance of considering multiple combined effects and responses of land biomes while reaching the global temperature targets of the Paris Agreement.

1 Introduction

The Paris Agreement, adopted under the Convention of the Parties of United Nations Framework Convention on Climate Change (UNFCCC) in 2015, aims to limit the temperature increase to 2°C, and strive for 1.5°C above pre-industrial levels (UNFCCC, 2015). This temperature target is very ambitious considering the rate of current warming as such goals require not only strong mitigation efforts (e.g., Rogelj et al., 2016, 2018; van Vuuren et al., 2018), but also application of negative emission technologies or carbon dioxide removal (CDR) (IPCC, 2018). Geoengineering has been discussed as a potential option to

offset the global impacts of anthropogenic climate change, and at the same time help reach the global temperature targets. The complex natural responses and consequences of such methods, however, should be fully understood before implementation of geoengineering to avoid any unexpected and potentially degrading impacts.

By definition, geoengineering is a deliberate attempt to modify the climate system on a sufficiently large scale to alleviate the impacts of climate change (Crutzen, 2006). Two broad categories of geoengineering, which have been discussed persistently in the Fifth Assessment Report of the Intergovernmental Panel on Climate Change (IPCC, 2013), are CDR and Solar Radiation Management (SRM). The CDR methods aim at capturing CO_2 from the atmosphere and storing it in reservoirs, where it stays isolated from the atmosphere for a significant period of time. This could be done in a number of different ways, from afforestation to direct air capture of CO_2 with long-term geological storage technology (Lawrence et al., 2018). The SRM methods, on the other hand, aim at modifying the atmospheric radiative budgets by reducing the amount of solar radiation reaching the Earth's surface to alleviate anthropogenic global warming. We hence refer to these methods as radiation management (RM) in this study following Schäfer et al. (2015).

Due to the long thermal inertia in the climate system and limitations in maximum removal rate of CO_2, CDR would likely require longer time to lower global temperatures (Zickfeld et al., 2017) compared to RM methods. On the other hand, several proposed RM methods could stabilize or even reduce global temperature within a few years (Lawrence et al., 2018). The benefits of RM methods may not only be in reducing the current rate of increase in atmospheric temperatures, but also in mitigating climate extremes likely caused by warming (Irvine et al., 2019). Despite this encouraging potential, studies have shown numerous undesirable climatic and biophysical side effects of RM particularly related to sudden termination of RM (e.g., Keller et al., 2014; Lauvset et al., 2017; Lee et al., 2019; Robock et al., 2009; Tjiputra et al., 2016). These studies point out that upon sudden termination of RM, the climate system will return to its "unmitigated" state within a few decades. This may lead to very large rates of change in the climatic state, unless there is a solution to reduce atmospheric CO_2 concentrations. Nevertheless, our understanding on how RM influence vegetation carbon (C) dynamics at regional scales remains limited, with only a few studies published, with focus on single or simplistic RM methods (Dagon and Schrag, 2019; Muri et al., 2014, 2018; Naik et al., 2003; Tjiputra et al., 2016; Xia et al., 2016; Yang et al., 2020; Zhang et al., 2019).

In this study, we assess the response of different terrestrial biomes in their ecosystem C exchange and storage under three different RM methods using an Earth System Model. There are a number of different methods studied within RM, including the aerosol injection based ones used in this study. The three RM methods considered in this study are stratospheric aerosol injection (SAI), marine sky brightening (MSB), and cirrus cloud thinning (CCT). The mechanisms how different methods stabilize the climate are quite different, where SAI and MSB regulate shortwave radiation and CCT modifies terrestrial radiation. Among the three, the most studied is SAI (e.g., Robock, 2016; Tilmes et al., 2015; Tjiputra et al., 2016), which involves increasing the backscatter of solar radiation to space by introducing an reflective aerosol layer in the stratosphere. Bright and reflective aerosols also form the foundation of another method; namely MCB (Ahlm et al., 2017; Alterskjær et al., 2013; Latham et al., 2012). The principle here is to inject aerosols such as sea salt into low cloud layers over the tropical oceans, to make these more effective at reflecting incoming radiation, hence reduce surface warming. If such spraying is done outside of the typical cloud deck areas, the brightness of the aerosols themselves may also cool the climate (Ahlm et al., 2017). Hence the term 'marine

sky brightening (MSB)' has been used in the literature (Schäfer et al., 2015; Ahlm et al., 2017), since the sky and not just the clouds are brightened. Furthermore, there is a less studied method referred to as CCT (Gasparini et al., 2020; Mitchell and Finnegan, 2009; Kristjánsson et al., 2015), which aims to cool by letting more longwave radiation escape to space by removing or thinning out high level ice clouds (cirrus clouds). This could also be done by seeding with aerosols. Since thinning of cirrus clouds primarily would act on the longwave range of the spectrum, as opposed to the other two aforementioned methods, we refer to the methods used in this study collectively as RM rather than the commonly used term SRM to be inclusive of CCT.

The modeling study by Muri et al. (2018) demonstrates that all three of these methods could potentially stabilize atmospheric temperature and reduce net radiative forcing on climate. Side effects, however, may persist as these methods alter atmospheric circulation and precipitation patterns. Studies from Geoengineering Model Intercomparison Project (GeoMIP, Kravitz et al. (2015)) demonstrate that there is substantial regional climate variation in response to different methods, scenarios, and models (e.g., Stjern et al., 2018; Wei et al., 2018; Yu et al., 2015). As a result, different terrestrial ecosystems exhibit varying patterns in vegetation production (net primary productivity, NPP). Analyses in vegetation responses show that global mean and high latitude NPP have different patterns (Jones et al., 2013; Lee et al., 2019). This is likely due to different RM methods resulting in different patterns of precipitation in particular. In addition to temperature and precipitation, different biomes are limited by different environmental factors, such as growing season length, dry season length, availability of sunlight for photosynthesis, and soil fertility.

This led us to investigate the following questions: 1) What are the key factors affecting future vegetation under different RM applications? 2) If there are regional differences in the environmental change under RM applications, which terrestrial biomes are affected the most in ecosystem C uptake and storage? 3) What is the impact of geoengineering termination on vegetation and terrestrial C storage? 4) What are the effects of RM applications in global vegetation compared to lower emissions and mitigation scenario (i.e. RCP4.5)?

1.1 Model description (NorESM)

We conducted three different aerosol-based geoengineering experiments using the fully coupled NorESM1-ME, where we investigated the impacts of idealized scenarios of aerosol-based geoengineering under a high-CO_2 RCP8.5 and the target temperature scenario RCP4.5 future scenarios. NorESM1-ME is based on the Community Earth System Model (CESM; Gent et al., 2011). Some of the key differences in NorESM1-ME from CESM are: (1) a more sophisticated tropospheric chemistry-aerosol-cloud scheme (Kirkevag et al., 2013), (2) a different ocean circulation model based on the Miami Isopycnic Coordinate Ocean Model (MICOM) with extensive modifications (Bentsen et al., 2013), and (3) the ocean biogeochemical model, which originated from the Hamburg Oceanic Carbon Cycle (HAMOCC) model (Tjiputra et al., 2013). Both the land and atmospheric components have a horizontal resolution of 1.9° latitude × 2.5° longitude, with 26 vertical levels in the atmosphere, whereas the ocean model employs a displaced pole grid with a nominal ~1° resolution with 53 isopycnal layers.

The land component of NorESM1-ME is CLM4 (Lawrence et al., 2011). The land C cycle module in CLM4 includes carbon-nitrogen (CN) coupling that is prognostic in CN as well as vegetation phenology. As a result, plant photosynthesis is also limited by the nitrogen (N) availability (Thornton et al., 2009). The CLM4 has separate state variables for C and N, which

are followed through separately in leaf, live stem, dead stem, live coarse root, dead coarse root, and fine root pools. There are two corresponding storage pools representing short-term and long-term storage of non-structural carbohydrates and labile N. Sources and sinks of mineral N are implemented in the form of atmospheric deposition, biological N fixation, denitrification, leaching, and losses due to fire events. The CLM4 photosynthesis uses both direct and diffuse radiation for sunlit leaves and only diffuse radiation for shaded leaves (Bonan et al., 2011). The plant functional types (PFTs) and land cover change distribution in CLM4 is prescribed and updated annually according to the Coupled Model Intercomparison Project phase 5 (CMIP5) global land use and land cover change dataset (Lawrence et al., 2011, 2012). The transient PFT and land cover fields take into account historical and future climate change under RCP8.5 scenario (1850-2100), which were implemented using the harmonized land use change scenarios and Integrated Assessment Model, respectively. Details on PFT, terrestrial C and N cycling, and land cover implementation in the CLM4 model are described in Lawrence et al. (2011). For this study, NorESM is run with a fully interactive prognostic C cycle (i.e. in emission driven mode).

1.2 Aerosol-based geoengineering experiments

Two of the RM methods used in this study aim to reduce the amount of solar radiation reaching the surface to alleviate global warming through spraying of aerosols into the atmosphere: SAI (e.g., Crutzen, 2006; Robock, 2016) and MSB (Ahlm et al., 2017; Latham, 1990). Another technique aims at increasing the amount of outgoing thermal radiation to space by reducing the cover of high level ice clouds: CCT (Storelvmo et al., 2013). Increasing application of RM was used to lower the total radiative forcing in the RCP8.5 baseline simulation down to a temperature level corresponding to RCP4.5, as described in Muri et al. (2018) and similar to the G6sulfur experiment of GeoMIP (Kravitz et al., 2015). The RM is started in year 2020 on the background of the RCP8.5 scenario and continued until the end of the century. The mean of three ensemble members were used for each case. In year 2101 the RM was ended. One ensemble member was extended for another 50 years for each case, such that effects of sudden termination of large-scale RM may be assessed.

The aerosol-based RM experiments were implemented as follows:

1.2.1 Stratospheric aerosol injections (RCP8.5 + SAI)

Since there is no interactive stratospheric aerosol scheme in NorESM1-ME, stratospheric aerosol properties were prescribed based on the approach of Tilmes et al. (2015), although different reference cases are used. In simulations with the ECHAM5 model, sulfur dioxide was released at ~2 km altitude (60 hPa) in a grid box at the equator. The interactive aerosol microphysics module within the general circulation model of ECHAM5 (Niemeier et al., 2011) calculated the resulting distribution of sulfate aerosols in the stratosphere. The aerosol optical depth and distribution represented by the zonal aerosol extinction, single-scattering albedo, and asymmetry factors, were implemented in NorESM1-ME, and are described in more detail in Niemeier and Timmreck (2015). A number of test runs were performed to establish how much aerosols were needed to offset the anthropogenic radiative forcing between RCP8.5 and RCP4.5. The resulting aerosol layer corresponds to equivalent emissions of 5 Tg(S) yr^{-1} in 2050, 10 Tg(S) yr^{-1} in 2075 and as much as 20 Tg(S) yr^{-1} in 2100.

1.2.2 Marine sky brightening (RCP8.5 + MSB)

The sea salt emissions parameterisation in NorESM1-ME is coupled to the cloud droplet number concentrations. In this way, the emissions of sea salt may interact with cloud processes, including brightening effects. Emissions of sea salt aerosols were uniformly increased between latitudes of ±45°. This follows the approach of Alterskjær et al. (2013) and the emissions are increased over a wider latitude band to achieve an effective radiative forcing of -4 W m^{-2} more readily. The medium sized aerosol bin has been found to be most efficient at brightening clouds in NorESM (Alterskjær and Kristjánsson, 2013). Aerosol emissions were hence increased for the accumulation mode size, with a dry number modal radius of 0.13 μm, geometric standard deviation of 1.59, corresponding to a dry effective radius of 0.22 μm. Sea salt emission increases were on the order of 460 Tg yr^{-1} at the end of the century.

1.2.3 Cirrus cloud thinning (RCP8.5 + CCT)

With regards to cirrus cloud thinning, the Muri et al. (2014) method was used. The fall speed of all ice crystals at temperatures below -38°C was increased. This is a typical temperature for homogeneous freezing to start occurring. The coverage of ice clouds in the CMIP5 ensemble was assessed by Li et al. (2012), and NorESM was found to perform reasonably compared to satellite observations and indeed one of the better-performing models. The terminal velocity of ice was increased by a factor of 10 by 2100, i.e. within the observational range (Gasparini et al., 2017; Mitchell, 1996).

1.2.4 Analysis of biomes

We follow the definition of different land biomes as in Tjiputra et al. (2016), where plant functional types (PFT) in the CLM4 that represent certain biomes are merged together (e.g. Boreal forest biome includes boreal needleleaf evergreen tree, boreal needleleaf deciduous tree, boreal broadleaf deciduous tree, and boreal broadleaf deciduous shrub PFTs in the CLM4). The biomes are static by taking a 20 year mean (1981-2000) of PFT distribution from the surface dataset. See Supplementary Information 1 for overall distribution of the biomes used in this study. We note that projected land use change characteristics are very different in RCP8.5 and RCP4.5 (Hurtt et al., 2011). While there is an increase in cropland and grassland (driven by food demand of an increasing population) at the expense of forested land in RCP8.5, there is an increasing area of forest due to assumed reforestation programs in the mitigation scenario RCP4.5 (van Vuuren et al., 2011).

2 Results and Discussion

2.1 Global scale responses under RM applications

The three RM methods alter the direct visible radiation (DVR) and diffuse visible radiation (FVR) in different directions, with little impact on the level of atmospheric CO_2 concentrations (Figure 1). The differences in direct and diffuse radiation is attributed to how the radiation management methods are implemented, where each differs in affecting longwave and shortwave radiation (Muri et al., 2018). Regardless of the methodological differences, all RM methods are able to reduce the net radiation

at the top of the atmosphere and the global mean air temperatures close to the RCP4.5 level as expected. Global land surface air temperature (TSA) increases at a slower rate until the end of the 21st century under all three RM scenarios compared to the baseline RCP8.5 scenario, where there is approximately 2.3°C difference between RM and non-RM world at year 2100. Under CCT application, the increase in global precipitation is somewhat higher than RCP8.5 as explained in Muri et al. (2018). CCT keeps the level of precipitation close to RCP8.5 until the year 2100 due to an amplified hydrological cycle from increased latent heat flux (Kristjánsson et al., 2015). CCT has been shown to lead to an increase in precipitation in previous studies (Jackson et al., 2016; Kristjánsson et al., 2015; Muri et al., 2018), where the radiative cooling of the troposphere increases the latent heat flux at the surface and hence alters the precipitation rates. SAI shows a reduced rate of increase in global precipitation similar to RCP4.5. Under MSB application, the rate of global precipitation increase falls in between the SAI and CCT.

There is a large overall increase in global mean NPP until the end of the 21st century in the RCP8.5 scenario and under the three RM scenarios (Figure 1), whereas only a small increase in NPP is simulated under the RCP4.5 scenario. At the same time, there is a large increase in the rate of soil organic matter decomposition (heterotrophic respiration: HR) in the RCP8.5 based experiments. Relatively small NPP differences are observed between RCP8.5 and the RM simulations compared to the RCP4.5 scenario. This illustrates that the CO_2 fertilization effect is much larger in regulating NPP than the effects of temperature and precipitation, as the level of temperature and (in the case of SAI and MSB) precipitation are similar between the RCP4.5 scenario and the three RM methods on a global scale.

2.2 Regional differences in temperature and precipitation

There are no discernable spatial patterns shown in the changes in direct and diffuse radiation except that changes in direct radiation under the CCT application are more concentrated in the tropics. The SAI method shows considerablely increased diffuse radiation throughout the global land areas compared to the baseline RCP8.5 scenario (Supplementary Information 2). While TSA exhibits similar patterns across different RM applications, the precipitation patterns are more variable over space across different RM methods. The global spatial patterns of precipitation towards the end of the century (mean of 2070-2100, Figure 2) show that CCT generally increases precipitation in the tropics and Mediterranean region relative to RCP8.5. In particular, MSB tends to increase precipitation over extratropical land more than SAI due to the regional application of the forcing (Alterskjær et al., 2012). The spatial patterns of precipitation change in MSB mostly follows that of CCT, but the magnitude of change is smaller. On the other hand, SAI shows overall decreases in precipitation particularly in the tropics relative to RCP8.5. All three methods show a decrease in precipitation in the East Asia region.

The differences in temperature and precipitation across the tree RM methods in different land biomes of the world show that there is no noticeable difference in mean annual temperature across the three different RM methods (Figure 3). The cooling imbalance across the three RM forcings exist, where the tropics tend to cool more than high latitudes and cooling is more pronounced in the ocean than on land, with a stronger southern hemispheric cooling for CCT (Muri et al., 2018). We show that precipitation patterns vary across the three methods in different biomes. In all biomes, SAI application results in the largest decrease in precipitation followed by MSB relative to RCP8.5 scenario. Under CCT application, precipitation even increases beyond the RCP8.5 level. The precipitation differences across the three methods are large, particularly in the tropics

and the mid-latitudes, where CCT application results in higher precipitation rates than the two other methods. The differences in precipitation are amplified over time until the end of the 21st century. According to Muri et al. (2018), shortwave radiation based geoengineering methods exhibit strong reduction in global precipitation levels relative to the RCP8.5, but also relative to the RCP4.5. CCT leads to a slight increase in global precipitation even over the RCP8.5 levels, however, land precipitation patterns in different biomes vary. Aggregated over all biomes, precipitation changes are much smaller than over the total (ocean+land) area. Particularly, precipitation is not reduced much below the RCP4.5 levels for SAI and MSB as in Muri et al. (2018) (compare their Figure 2 with Figure 1 in this study).

2.3 Biome specific C uptake and release rate

The spatial patterns and the magnitude of NPP change under the three methods show distinct differences. There are common spatial patterns in NPP decrease at the north western part of Amazonia, equatorial Africa, and eastern Asia in the three RM experiments (Figure 2). But overall, the large increase in NPP at Europe and equatorial South America particularly CCT experiment compensates the decreases elsewhere, hence creating a general lack of deviation as a whole from the RCP8.5 scenario (see Figure 1). It is clear from the comparison shown in precipitation (Figure 2) that the NPP changes are most correlated by the spatial changes in precipitation.

Under the CCT application, there is a strong increase in NPP in the tropics and the Mediterranean region, but decrease in East Asia. MSB does not show noticeable change except increased NPP in Eastern Amazonia. The spatial pattern of NPP in MSB is similar to CCT but the magnitude is smaller in MSB. There is a strong decrease in NPP under SAI application, particularly in the tropics. These overall patterns follow similar spatial patterns as the precipitation and are highly correlated as expected (Supplementary Information 3). The differences in NPP is dominated largely by three biomes: tropical forest, grass-shrubland, and temperate forest (Figure 4). NPP and HR in MSB and SAI simulations negatively deviate from the RCP8.5 simulation, whereas in CCT both remain at a similar level to the RCP8.5 in the tropical forest, grass-shrubland, and temperate forest likely due to increased precipitation level in these biomes. But since temperature is a stronger regulator of NPP and HR in high latitude biomes, CCT simulations also exhibit decreased NPP and HR there compared to the RCP8.5 scenario. Additionally, we do not observe any noticeable changes in seasonality for NPP and LAI between RM methods and RCP8.5 scenario (Supplementary Information 4 and 5) as seen in Dagon and Schrag (2019). Although there is spatial variability in precipitation patterns, there is no change in seasonality between the three RM methods and the baseline RCP8.5 scenario.

Overall, the varying precipitation patterns may be the strongest driver of the responses of global scale C uptake and release. Changes in diffuse radiation is found to affect photosynthesis (Keppel-Aleks and Washenfelder, 2016) as diffuse radiation can be more efficient in photosynthesis (e.g., Gu et al., 2002). Under these assumptions, increase in diffuse radiation and decrease in direct radiation under SAI is expected to increase plant photosynthesis (Mercado et al., 2009; Xia et al., 2016). Increases in diffuse radiation are known to positively affect photosynthesis upto a threshold of the ratio between diffuse and total radiation at around 0.4-0.45 (Knohl and Baldocchi, 2008; Mercado et al., 2009). Across the three RM methods, this ratio ranges from 0.29 (CCT) to 0.4 (SAI) at the end of the RM application in year 2100. The responses of NPP under changes in diffuse radiation on different RM applications exhibited in our study suggest that changes in diffuse radiation may not be the largest

driver of NPP change at the global level as much as temperature and precipitation. Under the coupled framework of ESM, it is very difficult to decompose the direct single effects of climatic factors due to interactions (Zhang et al., 2019) and separate simulations are necessary to directly quantify this. The N limitation implemented in the CLM4 has shown to limit C uptake by 74% relative to the C only model (Thornton et al., 2007), but CLM4 still exhibits NPP biases in the tropics (Lawrence et al., 2011). It is important to note that despite the strong CO_2 fertilization as well as increase in diffuse radiation, NPP in some parts of the tropics decreases under the SAI application likely due to the strong decrease in precipitation (Figure 2, Supplementary Information 3 and 4).

2.4   Biome specific C storage

Vegetation C storage in different biomes illustrate that global vegetation C storage changes are dominated by the responses in tropical forest biome (Figure 5). Under the baseline RCP8.5 scenario, global vegetation C storage decreases due to reduced tropical and temperate forest and grass-shrubland area as part of the land use change scenario used in the RCP8.5 scenario (Riahi et al., 2011). Compared to the baseline RCP8.5 scenario, vegetation C in Arctic tundra, boreal forest, and tropical forest biomes are affected the most under RM applications. In Arctic tundra and boreal forest biomes, all three RM scenarios result in a slightly reduced accumulation in vegetation C compared to RCP8.5 scenario likely due to decreased temperature exhibiting the temperature limitation in high latitude biomes. In tropical forest, SAI application reduces vegetation C storage relative to the RCP8.5 scenario, but CCT application slightly increases C storage due to increased precipitation (Figure 2). The magnitude of change in global vegetation C at the end of the century due to application of different RM methods are up to 10 PgC. On the other hand, the magnitude of vegetation C reduced due to the different underlying land use change scenarios in RCP4.5 and RCP8.5 is up to 100 PgC (Figure 5, Supplementary Information 7). These differences are attributed to increased forest and grassland area as part of the RCP4.5 scenario (Thomson et al., 2011). This highlights that large scale changes in vegetation C storage depends much more on anthropogenic land use change than on additional perturbations caused by application of RM in our simulations.

In tropical forest, the differences in vegetation C storage appeared to be correlated to precipitation patterns, where decrease and increase in precipitation in the three different methods regulate vegetation C storage. Differences in vegetation and soil C storage in temperate zone (temperate forest and grass-shrubland), however, did not always correspond directly to varying precipitation patterns. For instance, approximately 100-120 mm difference in mean annual precipitation shown in temperate forest and grass-shrubland biomes between SAI and CCT methods do not portray into differences in vegetation C storage (Figure 3, Supplementary Information 6).

2.5   Effects of RM termination

Upon sudden termination of RM applications, the level of radiation, temperature, and precipitation quickly converge to the baseline RCP8.5 scenario (Figures 1, 3, 4). Note that the temperature does not increase to exactly the same level as the RCP8.5 scenario, which has been observed in previous studies and is due to the thermal inertia of ocean heat uptake (Tjiputra et al., 2016). As the temperature and precipitation patterns converge towards the RCP8.5 scenario, NPP also becomes similar to the

255 RCP8.5 scenario (Figure 1). The soil C storage decreases as RM is terminated and towards the end of the simulation in year 2150, soil C storage in all three RM methods are at a similar level (Supplementary Information 6), but the magnitude is still higher than under the RCP8.5 scenario by 10 PgC globally. The likely accumulation of soil C under RM applications may be viewed as one of the positive effects of geoengineering, which was supported by a recent multimodel comparison study (Yang et al., 2020). Globally, land C accumulation associated with RM would remain on land for at least 50 years following

260 termination (Muri et al., 2018). Although the termination effects seem catastrophic due to its rapidity in particular, some studies suggest that realistically the most extreme cases would be unlikely as termination could be avoided by geopolitical agreement once deployed (Parker and Irvine, 2018).

2.6 Implications and limitations

Reduced atmospheric temperature and precipitation under RM have large effects on vegetation C storage compared to the base-
265 line scenario, RCP8.5. Under the RCP4.5 scenario, the rate of C uptake denoted as NPP is slower due to reduced temperature, precipitation, and atmospheric CO_2 levels (Figure 1). However, global vegetation C storage is far greater than the RCP8.5 and the three RM simulations, which are based on underlying RCP8.5 scenario assumptions (Figure 5), due to the larger forest and grassland areas in the RCP4.5 scenario (Thomson et al., 2011). As a result, the difference in global vegetation C between the RCP4.5 scenario and the rest of the RCP8.5 based scenarios is nearly 170 PgC. This strongly suggests that on a global scale,
270 the areal change of vegetation and land surface management play very important roles when accounting for the global scale vegetation C storage. We suggest taking this point into account when comparing the different pros and cons of technological applications such as geoengineering and mitigation options such as afforestation.

Our results suggest that even with reduced temperature stress created by RM applications, productivity of vegetation in the three most productive biomes on Earth may be reduced due to changing precipitation patterns (particularly SAI). Therefore,
275 considering the changes (i.e., reduction) in precipitation alone, RM may have negative effects on non-irrigated crops or food production globally. Nevertheless, the effects of CO_2 fertilization in the future are suggested to compensate for the deleterious impacts of both RM-induced temperature and precipitation changes (Pongratz et al., 2012; Xia et al., 2016). Although not directly investigated in this study, different RM methods have shown various climate extremes as well as mitigating them, which will have profound effects on the physiology of vegetation (Aswathy et al., 2015). Indeed, some studies show seasonal
280 variation in temperature under geoengineering (Dagon and Schrag, 2019), although we did not observe this in our study. This is not within the scope of our study, but could be an interesting point to consider in future studies.

We acknowledge that CLM4 has numerous limitations that prevents it from accurately estimating global scale soil C storage, and therefore, we do not make an estimation of global soil C storage. But here, we compare soil C storage under different methods to understand the factors controlling the difference across the three RM methods. Soil C storage increases under
285 RM applications compared to the baseline RCP8.5 scenario (Supplementary Information 6 and 7), because the decrease in temperature slows the rate of soil organic matter decomposition by microorganisms. An increase in total soil C is also simulated under the RCP4.5 scenario (Supplementary Information 7) likely due to the combination between increased vegetation C accumulation and slight reduction in soil respiration. There is an increase in soil C storage under RCP8.5 scenario early 21st

century due to increased NPP, but ultimately soil C decreases quickly due to excellerated soil respiration (Figure 1). In different biomes, temperate forest exhibits the largest difference across the three RM methods, where soil C storage under SAI method is nearly 1.0 PgC higher than CCT at the end of the 21st century. This is likely due to lower precipitation in SAI, which reduced the rate of decomposition.

3 Conclusions

We show that the three different RM applications mainly differ in the precipitation patterns, which in turn affect differences in global scale NPP. The precipitation differences across the three RM applications are the most pronounced in the tropics and mid-latitudes, where SAI application results in the largest decrease in precipitation followed by MSB, and CCT relative to RCP8.5 scenario. Tropical forest shows the largest variability in NPP and vegetation C storage as the precipitation patterns vary the most across the three methods in the tropics compared to other biomes. Ultimately, all three RM applications investigated in this study reduced the surface temperature to the level of RCP4.5 scenario with vegetation C uptake and storage being affected due to different temperature and precipitation patterns created by the different RM methods. Our results illustrate that there are regional differences in the biogeochemical cycles under application of large scale RM and suggest that such effects should be taken into consideration in future shaping of climate policies. Although changes in temperature and precipitation plays a large role in vegetation C storage capacity, CO_2 fertilization plays a considerable role in terrestrial C dynamics that can overshadow the effects of temperature and precipitation. Furthermore, changes in vegetation C storage under large-scale RM applications are much smaller than that exhibited under RCP4.5 scenario, which uses climate mitigation efforts by afforestation in the tropics. Hence, it would be important to consider the multiple combined effects and responses of land biomes when applying different strategies to reach the global temperature targets of the Paris Agreement.

Data availability. The model simulations used in this study are archived and available at the Norwegian Research Data Archive server (https://doi.org/10.11582/2019.00007).

Author contributions. HM and JT received funding; HM and JT designed and conducted simulations; HL and AE analyzed the data; HL, HM, and JS wrote the manuscript; all authors contributed to editing of the manuscript

Competing interests. There are no competing interests present.

Disclaimer. TEXT

Acknowledgements. This research was supported by the Research Council of Norway projects EXPECT (229760/E10), EVA (229771), and HiddenCosts (268243); Bjerknes Centre for Climate Research strategic project SKD-LOES. The simulations were performed on resources provided by UNINETT Sigma2 - the National Infrastructure for High Performance Computing and Data Storage in Norway, accounts nn9182k, nn9448k, NS2345K, and NS9033K.

315

References

Ahlm, L., Jones, A., Stjern, C. W., Muri, H., Kravitz, B., and Kristjánsson, J. E.: Marine cloud brightening - as effective without clouds, Atmospheric Chemistry and Physics, 17, 13 071–13 087, https://doi.org/10.5194/acp-17-13071-2017, 2017.

Alterskjær, K. and Kristjánsson, J. E.: The sign of the radiative forcing from marine cloud brightening depends on both particle size and injection amount, Geophysical Research Letters, 40, 210–215, https://doi.org/10.1029/2012GL054286, 2013.

Alterskjær, K., Kristjánsson, J. E., and Seland, O.: Sensitivity to deliberate sea salt seeding of marine clouds - observations and model simulations, Atmospheric Chemistry and Physics, 12, 2795–2807, https://doi.org/10.5194/acp-12-2795-2012, 2012.

Alterskjær, K., Kristjánsson, J. E., Boucher, O., Muri, H., Niemeier, U., Schmidt, H., Schulz, M., and Timmreck, C.: Sea-salt injections into the low-latitude marine boundary layer: The transient response in three Earth system models, Journal of Geophysical Research-Atmospheres, 118, 12 195–12 206, https://doi.org/10.1002/2013JD020432, 2013.

Aswathy, N., Boucher, O., Quaas, M., Niemeier, U., Muri, H., Muelmenstaedt, J., and Quaas, J.: Climate extremes in multi-model simulations of stratospheric aerosol and marine cloud brightening climate engineering, Atmospheric Chemistry and Physics, 15, 9593–9610, https://doi.org/10.5194/acp-15-9593-2015, 2015.

Bentsen, M., Bethke, I., Debernard, J. B., Iversen, T., Kirkevag, A., Seland, O., Drange, H., Roelandt, C., Seierstad, I. A., Hoose, C., and Kristjánsson, J. E.: The Norwegian Earth System Model, NorESM1-M - Part 1: Description and basic evaluation of the physical climate, Geoscientific Model Development, 6, 687–720, https://doi.org/10.5194/gmd-6-687-2013, 2013.

Bonan, G. B., Lawrence, P. J., Oleson, K. W., Levis, S., Jung, M., Reichstein, M., Lawrence, D. M., and Swenson, S. C.: Improving canopy processes in the Community Land Model version 4 (CLM4) using global flux fields empirically inferred from FLUXNET data, JOURNAL OF GEOPHYSICAL RESEARCH-BIOGEOSCIENCES, 116, https://doi.org/10.1029/2010JG001593, 2011.

Crutzen, P. J.: Albedo enhancement by stratospheric sulfur injections: A contribution to resolve a policy dilemma?, Climatic Change, 77, 211–219, https://doi.org/10.1007/s10584-006-9101-y, 2006.

Dagon, K. and Schrag, D. P.: Quantifying the effects of solar geoengineering on vegetation, Climatic Change, 153, 235–251, https://doi.org/10.1007/s10584-019-02387-9, 2019.

Gasparini, B., Munch, S., Poncet, L., Feldmann, M., and Lohmann, U.: Is increasing ice crystal sedimentation velocity in geoengineering simulations a good proxy for cirrus cloud seeding?, Atmospheric Chemistry and Physics, 17, 4871–4885, https://doi.org/10.5194/acp-17-4871-2017, 2017.

Gasparini, B., McGraw, Z., Storelvmo, T., and Lohmann, U.: To what extent can cirrus cloud seeding counteract global warming?, ENVIRONMENTAL RESEARCH LETTERS, 15, https://doi.org/10.1088/1748-9326/ab71a3, 2020.

Gent, P. R., Danabasoglu, G., Donner, L. J., Holland, M. M., Hunke, E. C., Jayne, S. R., Lawrence, D. M., Neale, R. B., Rasch, P. J., Vertenstein, M., Worley, P. H., Yang, Z.-L., and Zhang, M.: The Community Climate System Model Version 4, Journal of Climate, 24, 4973–4991, https://doi.org/10.1175/2011JCLI4083.1, 2011.

Gu, L., Baldocchi, D., Verma, S., Black, T., Vesala, T., Falge, E., and Dowty, P.: Advantages of diffuse radiation for terrestrial ecosystem productivity, JOURNAL OF GEOPHYSICAL RESEARCH-ATMOSPHERES, 107, https://doi.org/10.1029/2001JD001242, 2002.

Hurtt, G. C., Chini, L. P., Frolking, S., Betts, R. A., Feddema, J., Fischer, G., Fisk, J. P., Hibbard, K., Houghton, R. A., Janetos, A., Jones, C. D., Kindermann, G., Kinoshita, T., Goldewijk, K. K., Riahi, K., Shevliakova, E., Smith, S., Stehfest, E., Thomson, A., Thornton, P., van Vuuren, D. P., and Wang, Y. P.: Harmonization of land-use scenarios for the period 1500-2100: 600 years of global gridded annual land-

use transitions, wood harvest, and resulting secondary lands, Climatic Change, 109, 117–161, https://doi.org/10.1007/s10584-011-0153-2, 2011.

IPCC: Climate Change: The Physical Science Basis. Contribution of Working Group I to the Fifth Assessment Report of the Intergovernmental Panel on Climate Change, edited by: Stocker, T. F., Qin, D., Plattner, G.-K., Tignor, M., Allen, S. K., Boschung, J., Nauels, A., Xia, Y., Bex, V., and Midgley, P. M., Cambridge University Press, Cambridge, UK and New York, NY, USA,, 2013.

IPCC: Global warming of 1.5°C. An IPCC Special Report on the impacts of global warming of 1.5°C above pre-industrial levels and related global greenhouse gas emission pathways, in the context of strengthening the global response to the threat of climate change, sustainable development, and efforts to eradicate poverty, V. Masson-Delmotte V., Zhai P., Pörtner H.O., Roberts D., Skea J., Shukla P.R., Pirani A., Moufouma-Okia W., Péan C., Pidcock R., Connors S., Matthews J.B.R., Chen Y., Zhou X., Gomis M.I., Lonnoy E., Maycock M., Tignor M., Waterfield T. (eds.), 2018.

Irvine, P., Emanuel, K., He, J., Horowitz, L. W., Vecchi, G., and Keith, D.: Halving warming with idealized solar geoengineering moderates key climate hazards, Nature Climate Change, 9, 295–299, https://doi.org/10.1038/s41558-019-0398-8, 2019.

Jackson, L. S., Crook, J. A., and Forster, P. M.: An intensified hydrological cycle in the simulation of geoengineering by cirrus cloud thinning using ice crystal fall speed changes, JOURNAL OF GEOPHYSICAL RESEARCH-ATMOSPHERES, 121, 6822–6840, https://doi.org/10.1002/2015JD024304, 2016.

Jones, A., Haywood, J. M., Alterskjær, K., Boucher, O., Cole, J. N. S., Curry, C. L., Irvine, P. J., Ji, D., Kravitz, B., Kristjánsson, J. E., Moore, J. C., Niemeier, U., Robock, A., Schmidt, H., Singh, B., Tilmes, S., Watanabe, S., and Yoon, J.-H.: The impact of abrupt suspension of solar radiation management (termination effect) in experiment G2 of the Geoengineering Model Intercomparison Project (GeoMIP), Journal of Geophysical Research-Atmospheres, 118, 9743–9752, https://doi.org/10.1002/jgrd.50762, 2013.

Keller, D. P., Feng, E. Y., and Oschlies, A.: Potential climate engineering effectiveness and side effects during a high carbon dioxide-emission scenario, Nature Communications, 5, 3304, https://doi.org/10.1038/ncomms4304, 2014.

Keppel-Aleks, G. and Washenfelder, R. A.: The effect of atmospheric sulfate reductions on diffuse radiation and photosynthesis in the United States during 1995-2013, GEOPHYSICAL RESEARCH LETTERS, 43, 9984–9993, https://doi.org/10.1002/2016GL070052, 2016.

Kirkevag, A., Iversen, T., Seland, O., Hoose, C., Kristjánsson, J. E., Struthers, H., Ekman, A. M. L., Ghan, S., Griesfeller, J., Nilsson, E. D., and Schulz, M.: Aerosol-climate interactions in the Norwegian Earth System Model-NorESM1-M, Geoscientific Model Development, 6, 207–244, https://doi.org/10.5194/gmd-6-207-2013, 2013.

Knohl, A. and Baldocchi, D. D.: Effects of diffuse radiation on canopy gas exchange processes in a forest ecosystem, JOURNAL OF GEOPHYSICAL RESEARCH-BIOGEOSCIENCES, 113, https://doi.org/10.1029/2007JG000663, 2008.

Kravitz, B., Robock, A., Tilmes, S., Boucher, O., English, J. M., Irvine, P. J., Jones, A., Lawrence, M. G., MacCracken, M., Muri, H., Moore, J. C., Niemeier, U., Phipps, S. J., Sillmann, J., Storelvmo, T., Wang, H., and Watanabe, S.: The Geoengineering Model Intercomparison Project Phase 6 (GeoMIP6): simulation design and preliminary results, Geoscientific Model Development, 8, 3379–3392, https://doi.org/10.5194/gmd-8-3379-2015, wOS:000364326200024, 2015.

Kristjánsson, J. E., Muri, H., and Schmidt, H.: The hydrological cycle response to cirrus cloud thinning, Geophysical Research Letters, 42, 10 807–10 815, https://doi.org/10.1002/2015GL066795, 2015.

Latham, J.: Control of Global Warming, Nature, 347, 339–340, https://doi.org/10.1038/347339b0, 1990.

Latham, J., Bower, K., Choularton, T., Coe, H., Connolly, P., Cooper, G., Craft, T., Foster, J., Gadian, A., Galbraith, L., Iacovides, H., Johnston, D., Launder, B., Leslie, B., Meyer, J., Neukermans, A., Ormond, B., Parkes, B., Rasch, P., Rush, J., Salter, S., Stevenson,

T., Wang, H., Wang, Q., and Wood, R.: Marine cloud brightening, PHILOSOPHICAL TRANSACTIONS OF THE ROYAL SOCIETY A-MATHEMATICAL PHYSICAL AND ENGINEERING SCIENCES, 370, 4217–4262, https://doi.org/10.1098/rsta.2012.0086, 2012.

Lauvset, S. K., Tjiputra, J., and Muri, H.: Climate engineering and the ocean: effects on biogeochemistry and primary production, Biogeosciences, 14, 5675–5691, https://doi.org/10.5194/bg-14-5675-2017, wOS:000418333700001, 2017.

395 Lawrence, D. M., Oleson, K. W., Flanner, M. G., Thornton, P. E., Swenson, S. C., Lawrence, P. J., Zeng, X., Yang, Z.-L., Levis, S., Sakaguchi, K., Bonan, G. B., and Slater, A. G.: Parameterization improvements and functional and structural advances in version 4 of the Community Land Model, Journal of Advances in Modeling Earth Systems, 3, 10.1029/2011MS000 045, https://doi.org/10.1029/2011MS000045, 2011.

Lawrence, D. M., Oleson, K. W., Flanner, M. G., Fletcher, C. G., Lawrence, P. J., Levis, S., Swenson, S. C., and Bonan, G. B.: The CCSM4 land simulation, 1850-2005: Assessment of surface climate and new capabilities, Journal of Climate, 25, 2240–2260,
400 https://doi.org/10.1175/JCLI-D-11-00103.1, 2012.

Lawrence, M. G., Schaefer, S., Muri, H., Scott, V., Oschlies, A., Vaughan, N. E., Boucher, O., Schmidt, H., Haywood, J., and Scheffran, J.: Evaluating climate geoengineering proposals in the context of the Paris Agreement temperature goals, Nature Communications, 9, 3734, https://doi.org/10.1038/s41467-018-05938-3, 2018.

Lee, H., Ekici, A., Tjiputra, J., Muri, H., Chadburn, S. E., Lawrence, D. M., and Schwinger, J.: The response of permafrost
405 and high-latitude ecosystems under large-scale stratospheric aerosol injection and its termination, Earth's Future, 7, 605–614, https://doi.org/https://doi.org/10.1029/2018EF001146, 2019.

Li, J.-L. F., Waliser, D. E., Chen, W.-T., Guan, B., Kubar, T., Stephens, G., Ma, H.-Y., Deng, M., Donner, L., Seman, C., and Horowitz, L.: An observationally based evaluation of cloud ice water in CMIP3 and CMIP5 GCMs and contemporary reanalyses using contemporary satellite data, Journal of Geophysical Research-Atmospheres, 117, D16 105, doi:10.1029/2012JD017 640,
410 https://doi.org/10.1029/2012JD017640, 2012.

Mercado, L. M., Bellouin, N., Sitch, S., Boucher, O., Huntingford, C., Wild, M., and Cox, P. M.: Impact of changes in diffuse radiation on the global land carbon sink, Nature, 458, 1014–U87, https://doi.org/10.1038/nature07949, 2009.

Mitchell, D.: Use of mass- and area-dimensional power laws for determining precipitation particle terminal velocities, Journal of the Atmospheri Sciences, 53, 1710–1723, https://doi.org/10.1175/1520-0469(1996)053<1710:UOMAAD>2.0.CO;2, 1996.

415 Mitchell, D. L. and Finnegan, W.: Modification of cirrus clouds to reduce global warming, ENVIRONMENTAL RESEARCH LETTERS, 4, https://doi.org/10.1088/1748-9326/4/4/045102, 2009.

Muri, H., Kristjánsson, J. E., Storelvmo, T., and Pfeffer, M. A.: The climatic effects of modifying cirrus clouds in a climate engineering framework, Journal of Geophysical Research-Atmospheres, 119, 4174–4191, https://doi.org/10.1002/2013JD021063, 2014.

Muri, H., Tjiputra, J., Otterå, O. H., Adakudlu, M., Lauvset, S. K., Grini, A., Schulz, M., Niemeier, U., and Kristjánsson, J. E.: Climate
420 response to aerosol geoengineering: A multimethod comparison, J. Climate, 31, 6319–6340, https://doi.org/10.1175/JCLI-D-17-0620.1, 2018.

Naik, V., Wuebbles, D., DeLucia, E., and Foley, J.: Influence of geoengineered climate on the terrestrial biosphere, Environmental Management, 32, 373–381, https://doi.org/10.1007/s00267-003-2993-7, 2003.

Niemeier, U. and Timmreck, C.: What is the limit of climate engineering by stratospheric injection of SO2?, Atmospheric Chemistry and
425 Physics, 15, 9129–9141, https://doi.org/10.5194/acp-15-9129-2015, 2015.

Niemeier, U., Schmidt, H., and Timmreck, C.: The dependency of geoengineered sulfate aerosol on the emission strategy, Atmospheric Science Letters, 12, 189–194, https://doi.org/10.1002/asl.304, 2011.

Parker, A. and Irvine, P. J.: The Risk of Termination Shock From Solar Geoengineering, Earth's Future, 6, 456–467, https://doi.org/10.1002/2017EF000735, 2018.

430 Pongratz, J., Lobell, D. B., Cao, L., and Caldeira, K.: Crop yields in a geoengineered climate, NATURE CLIMATE CHANGE, 2, 101–105, https://doi.org/10.1038/NCLIMATE1373, 2012.

Riahi, K., Rao, S., Krey, V., Cho, C., Chirkov, V., Fischer, G., Kindermann, G., Nakicenovic, N., and Rafaj, P.: RCP 8.5—A scenario of comparatively high greenhouse gas emissions, Climatic Change, 109, 33. https://doi.org/10.1007/s10 584–011–0149–y, https://doi.org/10.1007/s10584-011-0149-y, 2011.

435 Robock, A.: Albedo enhancement by stratospheric sulfur injections: More research needed, Earth's Future, 4, 644–648, https://doi.org/10.1002/2016EF000407, 2016.

Robock, A., Marquardt, A., Kravitz, B., and Stenchikov, G.: Benefits, risks, and costs of stratospheric geoengineering, Geophysical Research Letters, 36, L19 703, doi:10.1029/2009GL039 209, https://doi.org/10.1029/2009GL039209, 2009.

Rogelj, J., den Elzen, M., Hoehne, N., Fransen, T., Fekete, H., Winkler, H., Chaeffer, R. S., Ha, F., Riahi, K., and Mein-
440 shausen, M.: Paris Agreement climate proposals need a boost to keep warming well below 2 degrees C, Nature, 534, 631–639, https://doi.org/10.1038/nature18307, wOS:000378676000026, 2016.

Rogelj, J., Popp, A., Calvin, K. V., Luderer, G., Emmerling, J., Gernaat, D., Fujimori, S., Strefler, J., Hasegawa, T., Marangoni, G., Krey, V., Kriegler, E., Riahi, K., van Vuuren, D. P., Doelman, J., Drouet, L., Edmonds, J., Fricko, O., Harmsen, M., Havlik, P., Humpenoeder, F., Stehfest, E., and Tavoni, M.: Scenarios towards limiting global mean temperature increase below 1.5 degrees C, Nature Climate Change,
445 8, 325–332, https://doi.org/10.1038/s41558-018-0091-3, 2018.

Schäfer, S., Lawrence, M., Stelzer, H., Born, W., and Low, S.: The European Transdisciplinary Assessment of Climate Engineer-ing(EuTRACE),Final Rep. of the FP7 CSA Project EuTRACE, Tech. rep., Institute for Advanced Sustainability Studies (IASS), Potsdam, Germany, 2015.

Stjern, C. W., Muri, H., Ahlm, L., Boucher, O., Cole, J. N. S., Ji, D., Jones, A., Haywood, J., Kravitz, B., Lenton, A., Moore, J. C., Niemeier,
450 U., Phipps, S. J., Schmidt, H., Watanabe, S., and Kristjánsson, J. E.: Response to marine cloud brightening in a multi-model ensemble, Atmospheric Chemistry and Physics, 18, 621–634, https://doi.org/10.5194/acp-18-621-2018, 2018.

Storelvmo, T., Kristjánsson, J. E., Muri, H., Pfeffer, M., Barahona, D., and Nenes, A.: Cirrus cloud seeding has potential to cool climate, Geophysical Research Letters, 40, 178–182, https://doi.org/10.1029/2012GL054201, 2013.

Thomson, A. M., Calvin, K. V., Smith, S. J., Kyle, G. P., Volke, A., Patel, P., Delgado-Arias, S., Bond-Lamberty, B., Wise, M. A.,
455 Clarke, L. E., and Edmonds, J. A.: RCP4.5: a pathway for stabilization of radiative forcing by 2100, Climatic Change, 109, 77–94, https://doi.org/10.1007/s10584-011-0151-4, 2011.

Thornton, P. E., Doney, S. C., Lindsay, K., Moore, J. K., Mahowald, N., Randerson, J. T., Fung, I., Lamarque, J. F., Feddema, J. J., and Lee, Y. H.: Carbon-nitrogen interactions regulate climate-carbon cycle feedbacks: results from an atmosphere-ocean general circulation model, Biogeosciences, 6, 2099–2120, https://doi.org/10.5194/bg-6-2099-2009, 2009.

460 Thornton, P. E., Lamarque, J.-F., Rosenbloom, N. A., and Mahowald, N. M.: Influence of carbon-nitrogen cycle cou-pling on land model response to CO2 fertilization and climate variability, GLOBAL BIOGEOCHEMICAL CYCLES, 21, https://doi.org/10.1029/2006GB002868, 2007.

Tilmes, S., Mills, M. J., Niemeier, U., Schmidt, H., Robock, A., Kravitz, B., Lamarque, J. F., Pitari, G., and English, J. M.: A new Geoengi-neering Model Intercomparison Project (GeoMIP) experiment designed for climate and chemistry models, Geoscientific Model Develop-
465 ment, 8, 43–49, https://doi.org/10.5194/gmd-8-43-2015, 2015.

Tjiputra, J. F., Roelandt, C., Bentsen, M., Lawrence, D. M., Lorentzen, T., Schwinger, J., Seland, O., and Heinze, C.: Evaluation of the carbon cycle components in the Norwegian Earth System Model (NorESM), Geoscientific Model Development, 6, 301–325, https://doi.org/10.5194/gmd-6-301-2013, 2013.

Tjiputra, J. F., Grini, A., and Lee, H.: Impact of idealized future stratospheric aerosol injection on the large-scale ocean and land carbon cycles, Journal of Geophysical Research-Biogeosciences, 121, 2–27, https://doi.org/10.1002/2015JG003045, 2016.

UNFCCC: Adoption of the Paris Agreement United Nations Framework Convention on Climate Change, Geneva: United Nations Office, 2015.

van Vuuren, D. P., Edmonds, J., Kainuma, M., Riahi, K., Thomson, A., Hibbard, K., Hurtt, G. C., Kram, T., Krey, V., Lamarque, J.-F., Masui, T., Meinshausen, M., Nakicenovic, N., Smith, S. J., and Rose, S. K.: The representative concentration pathways: an overview, Climatic Change, 109, 5–31, https://doi.org/10.1007/s10584-011-0148-z, 2011.

van Vuuren, D. P., Stehfest, E., Gernaat, D. E. H. J., van den Berg, M., Bijl, D. L., de Boer, H. S., Daioglou, V., Doelman, J. C., Edelenbosch, O. Y., Harmsen, M., Hof, A. F., and van Sluisveld, M. A. E.: Alternative pathways to the 1.5 degrees C target reduce the need for negative emission technologies, Nature Climate Change, 8, 391–397, https://doi.org/10.1038/s41558-018-0119-8, 2018.

Wei, L., Ji, D., Miao, C., Muri, H., and Moore, J. C.: Global streamflow and flood response to stratospheric aerosol geoengineering, Atmospheric Chemistry and Physics, 18, 16 033–16 050, https://doi.org/10.5194/acp-18-16033-2018, 2018.

Xia, L., Robock, A., Tilmes, S., and Neely III, R. R.: Stratospheric sulfate geoengineering could enhance the terrestrial photosynthesis rate, Atmospheric Chemistry and Physics, 16, 1479–1489, https://doi.org/10.5194/acp-16-1479-2016, 2016.

Yang, C.-E., Hoffman, F. M., Ricciuto, D. M., Tilmes, S., Xia, L., MacMartin, D. G., Kravitz, B., Richter, J. H., Mills, M., and Fu, J. S.: Assessing terrestrial biogeochemical feedbacks in a strategically geoengineered climate, Environmental Research Letters, 15, 104 043, https://doi.org/10.1088/1748-9326/abacf7, 2020.

Yu, X., Moore, J. C., Cui, X., Rinke, A., Ji, D., Kravitz, B., and Yoon, J.-H.: Impacts, effectiveness and regional inequalities of the GeoMIP G1 to G4 solar radiation management scenarios, Global and Planetary Change, 129, 10–22, https://doi.org/10.1016/j.gloplacha.2015.02.010, 2015.

Zhang, Y., Goll, D., Bastos, A., Balkanski, Y., Boucher, O., Cescatti, A., Collier, M., Gasser, T., Ghattas, J., Li, L., Piao, S., Viovy, N., Zhu, D., and Ciais, P.: Increased Global Land Carbon Sink Due to Aerosol-Induced Cooling, GLOBAL BIOGEOCHEMICAL CYCLES, 33, 439–457, https://doi.org/10.1029/2018GB006051, 2019.

Zickfeld, K., Solomon, S., and Gilford, D. M.: Centuries of thermal sea-level rise due to anthropogenic emissions of short-lived greenhouse gases, Proc Natl Acad Sci USA, 114, 657, https://doi.org/10.1073/pnas.1612066114, 2017.
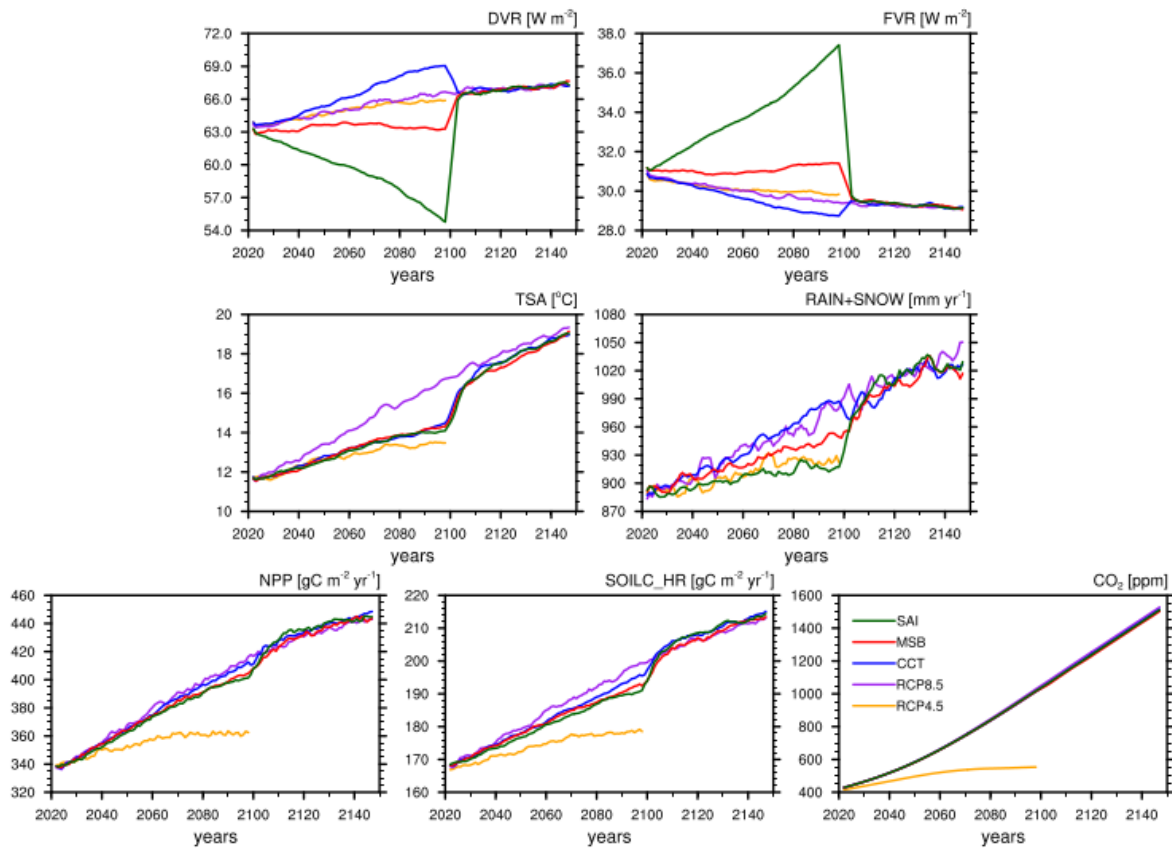
Figure 1. Time-series of land surface direct visible solar radiation (DVR), diffuse visible solar radiation (FVR), 2m air temperature (TSA), precipitation (RAIN+SNOW), net primary production (NPP), heterotrophic soil respiration (SOILC_HR), and atmospheric CO_2 from RCP4.5, RCP8.5, CCT, MSB, and SAI experiments. The values are spatial means over the land area between $60°$S and $70°$N latitudes.
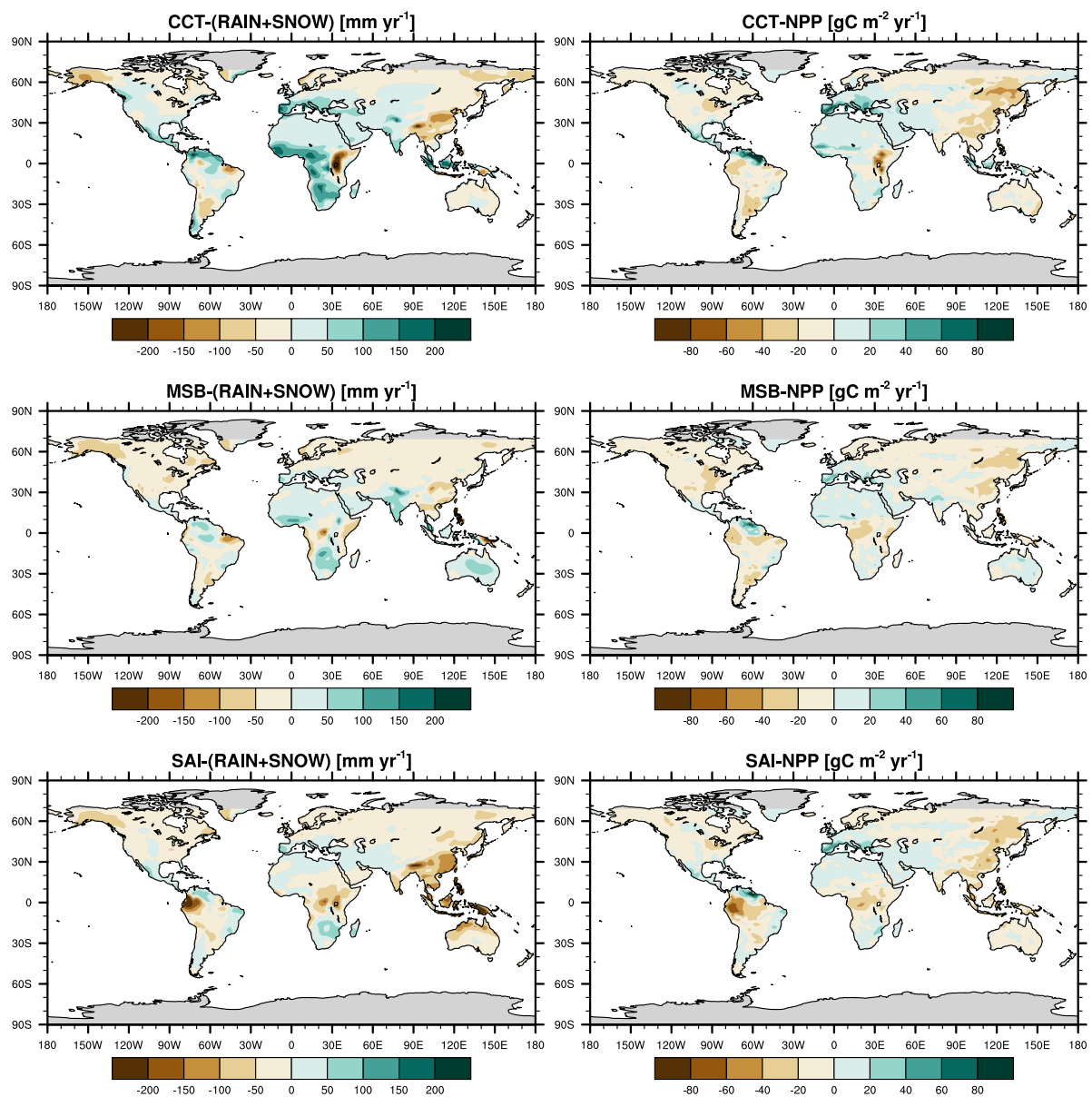
Figure 2. The deviation of precipitation and NPP simulated by CCT, MSB, and SAI relative to the baseline RCP8.5 scenario. The values shown here are the mean difference of the 2070-2100 time period and the mean over three ensemble members.
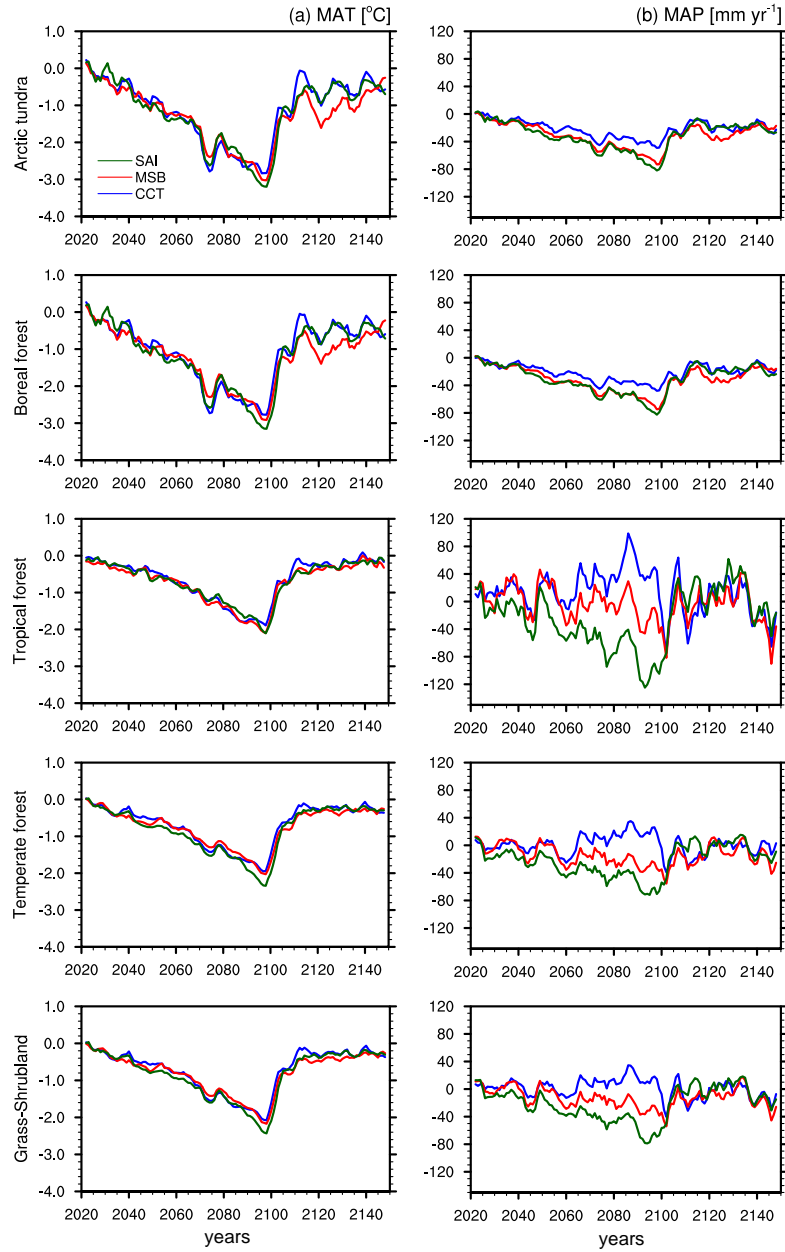
Figure 3. Mean annual temperature and precipitation in five different land biomes existing from -60 to 70°N latitude. The changes are relative to the baseline RCP8.5 scenario.
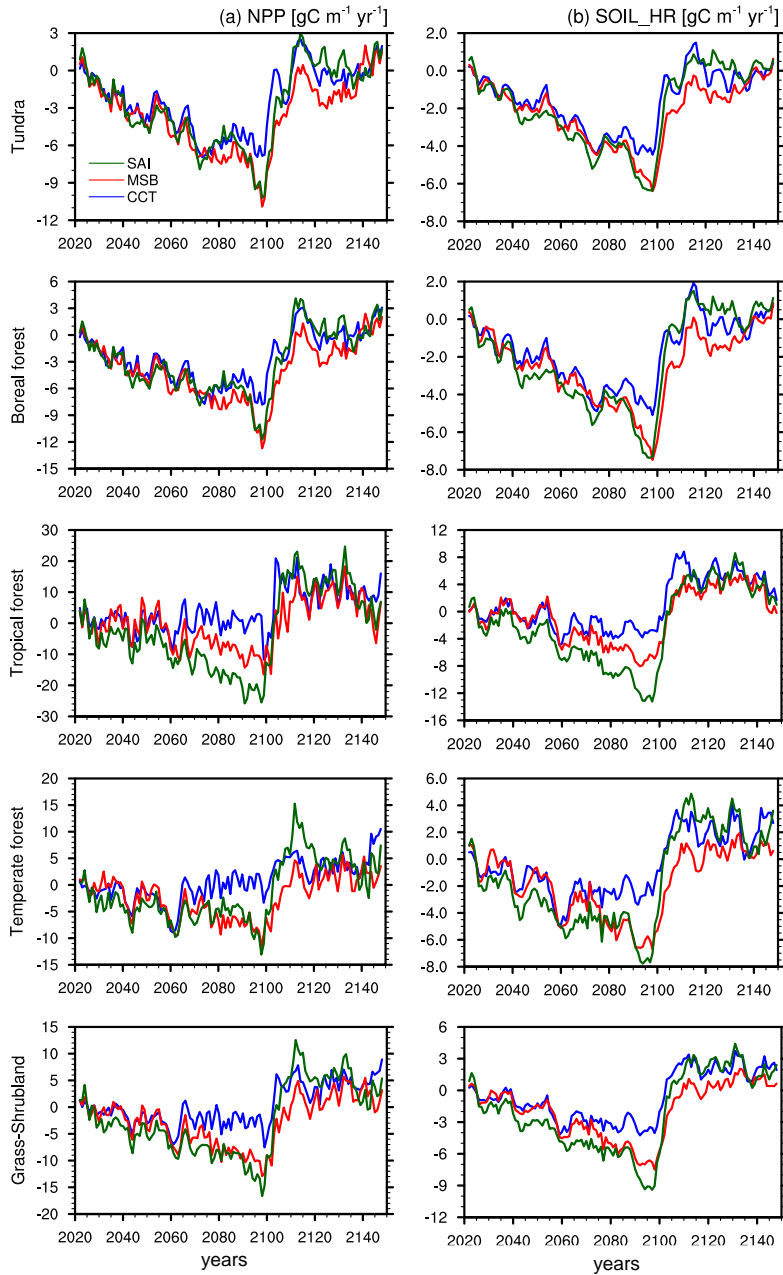
Figure 4. The relative difference between the RM to RCP8.5 scenario. The values are mean biome NPP and SOIL_HR in land areas across -60 to 70°N latitude. Note the different scales used in each panel.
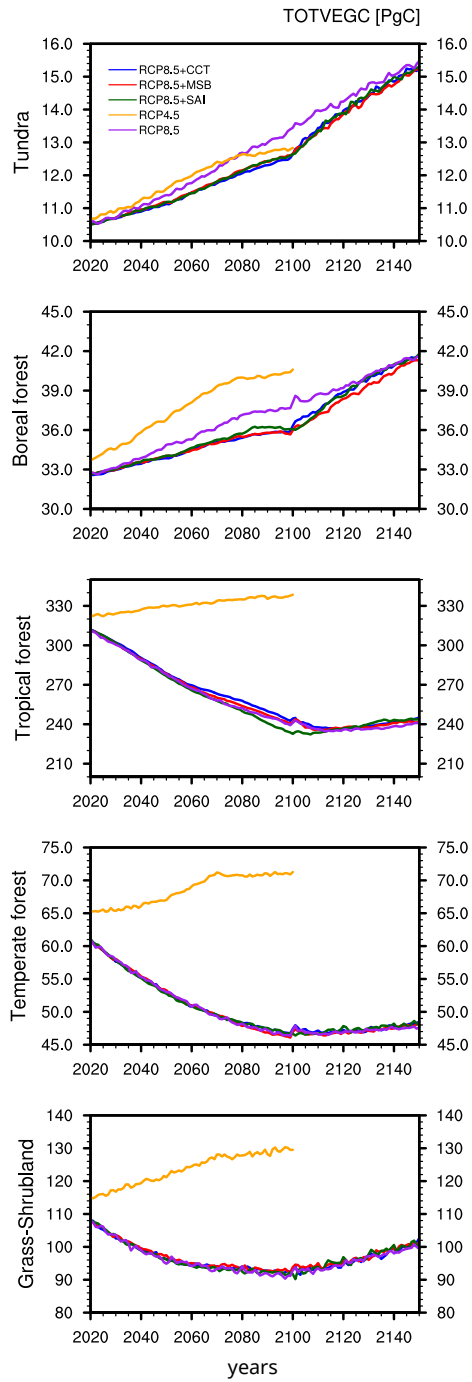
Figure 5. Total vegetation carbon storage in five different biomes under simulations of RCP8.5, three RM methods applied on top of RCP8.5 climate forcing (CCT, MSB, and SAI), and RCP4.5 scenarios.